QUERCETIN LOADED MAGNETITE NANOPARTICLES FOR METASTATIC BREAST CANCER

Gunjan Tiwari¹, Arun Radhakrishnan², Vikesh Kumar Shukla^{1*}

¹Department of Pharmaceutics, Amity Institute of Pharmacy, Amity University, Noida, Uttar Pradesh.

²Department of Pharmaceutics, JSS College of Pharmacy, Tamil Nadu.

^{*}Corresponding Author: Dr. Vikesh Kumar Shukla

Associate Professor, Department of Pharmaceutical Science, Amity Institute of Pharmacy, Amity University, Noida,

Uttar Pradesh.

e-mail: vkshukla@amity.edu, vikeshg2002@gmail.com

DOI: 10.47750/pnr.2022.13.S09.829

Abstract

Breast cancer is the most prevalence cancers in women and 1.67 million new cases of breast cancer were diagnosed. Quercetin is an active antioxidant flavonoid that can protect low-density lipoproteins from free radicals and it also possess pro-oxidant activity which could be used to treat metastatic breast cancer. In this work, we have formulated the magnetite nanoparticles loaded with quercetin for metastatic breast cancer with help of arbitrary interface of DOE for optimization. The developed MNP formulation's physiochemical characterization was found to be sufficient. The *in vitro* drug release study showed an initial release (48.55±2.09%) within 90 minutes, followed by a sustained drug release (99.35±4.58%) profile at the end of 87th hours and the kinetics of the *in vitro* release was calculated. The *in vitro* compatibility with MCF-7 cells showed that the quercetin loaded MNP was compatible and IC50 value 32μg/ml. These findings suggest that the quercetin loaded MNP has anticancer potential against metastatic breast cancer and they may be explored further for their effect through *in vivo* studies.

Keywords: Breast cancer; Quercetin; magnetite nanoparticle (MNP); DOE.

1. INTRODUCTION:

Breast cancer (BC) is the most prevalence cancers in women. Annually, worldwide around 1.67 million new cases of breast cancer were diagnosed, which accounts for 25% of all cancers diagnosed. Between 20% and 30% of breast cancer patients will develop simultaneous /metachronous distant metastatic stage, resulting in 500,000 deaths approximately in a year globally. In United States, the women with BC around 3.5% have distant metastatic disease at the time of their initial diagnosis, and this percentage is higher in low- and middle-income countries. This implies that about 50,000 women will be diagnosed with metastatic breast cancer for the first time each year ^[1]. Patients with BC have a relatively high 5-year survival rate when compared to other malignant tumors, but it drops dramatically when distant metastases are present ^[2]. A review of data from the Monitoring, Epidemiology, and Final Outcome database revealed that metastatic breast cancer (MBC) is extremely prevalent in mid- or elderly patients, with 63.7% occurring between the ages of 50 and 69, and 31.2% occurring over the age of 70 ^[3]. There is currently no cure for MBC; the primary treatment objectives are to relieve symptoms and prolong survival while minimizing toxicity and preserving quality of life. These factors are critical in the management of MBC in elderly women, who may have concomitant conditions and endure toxic treatments less well than their younger peers. When chemotherapy is needed, a sequential single strategy is the most appropriate therapeutic strategy to preserve

life quality and reduce the possibility of toxicity, whereas a combination of therapies has been shown to be too toxic and has no effect on overall survival [4]. Quercetin (Qu) is an active antioxidant flavonoid that can protect low-density lipoproteins from free radicals. As a result, the capacity of Qu could be beneficial against cancer cells. Several studies have used Qu as both an antioxidant and a pro-oxidant agent. Actually, the anti-oxidant or prooxidant activity is determined by the redox state of the cells as well as the concentration of Qu. The conclusive evidences show that Qu has low antioxidant activity and high pro-oxidant activity. By similarity with widely accepted anticancer drugs such as doxorubicin, the antioxidant and pro-oxidant properties of Qu have elevated cancer repression by producing oxidative stress. Qu is a component that inhibits the proliferation of several human BC-related cell lines [5]. Qu contributes to tumour growth prevention due to its pro-oxidant ability. Qu, at a same time, stimulates apoptosis and causes cell cycle arrest. The ultimate goal of cancer therapy is to induce apoptosis, and Qu's innate ability to induce apoptosis makes it a candidate for cancer probes [6]. Because of the benefits of specific targeting, decreased drug toxic effects, and substantially improved drug availability, nano-drug delivery systems (NDDS) have been successfully implemented to medical diagnosis and treatment. According to research, delivering chemotherapeutic drugs to tumor tissues using NDDS can effectively induce tumor killing, making it an effective strategy for treating breast cancer [7]. The ultrafine size, monodispersed structure, customized surfaces, colloidal stability, improved magnetization, cellular uptake, and bio-distribution of superparamagnetic nanoparticles are major factors for their application in biomedical applications. These properties make magnetic nanoparticles more useful for drug delivery, cell separation, protein separation, water purification, hyperthermia, diagnostics, and MRI contrast agents, among other things [8]. Magnetite, one of several iron oxides and a part of the spinel group, is a ferrimagnetic mineral type of iron (II, III) oxide (Fe3O4). Magnetite is a popular iron oxide mineral named after an ancient Greek region known for metal production. Magnetite nanoparticles (MNP) have received a lot of interest in the biomedical field, not only because of their magnetic properties, but also because of their biocompatibility. The field of bioassays has been a significant area of application, where the magnetic characteristics of the nanoparticles are used in vitro to modify the nanomaterials with an externally applied magnetic field [9]. The magnetite nanoparticles were up taken by the cancer cells and the internalized were distributed throughout the cell's components and almost every cell. This kind of formulation demonstrated very little macrophage absorption, which supports longer circulation times for a more potent treatment. The nanoparticle(s) effectively target cancer cells due to their high affinity, which enables preferential uptake through receptor-mediated endocytosis [10].

A statistical technique called design of experiments (DOE), which is a component of Quality by Construct (QbD), will systematically design new trials based on the scant quantity of experimental data that is now available [11]. The experiments are planned using the suitable in silico statistical tools. Defining the stated objective, parameterizing the component elements, doing an effect analysis, and looking at the predetermined replies are the steps in the process [12]. By evaluating the impacts of multiple dependent and independent characteristics on the provided responses, this technique has the essential advantage of making it possible to find correlations and interactions. The quality target product profile (QTPP), the quality risk assessment (QRA), the critical quality attributes (CQAs), and the design of experiments (DOE) are the tools used in quality by design [13]. A class of second-order designs known as Box-Behnken designs (BBD) that are rotatable or nearly rotatable are based on three-level incomplete factorial designs [14]. The main methods used by DOE to determine and interpret the design space are Response Surface Methodology (RSM) and Contour plot [15]. In this study, we have optimized the MNP using the arbitrary interface of DOE & formulated using co-precipitation method for the preparation of iron oxide and drug loaded MNP by ionic gelation method and evaluation of the prepared MNP was performed.

2. MATERIALS AND METHODS

2.1 Materials

2.2 Design of Experiment

By using Design Expert Software (Version 13.0.1.0), in silico modelling and evaluation were carried out. The Box-Behnken design (BBD) was chosen for this project, and various formulation parameters were chosen as

independent variables based on the screening using factorial design. The particle size and zeta potential of the MNP were taken into account as dependent variables, with the zeta potential indicating the integrity of MNP.

2.3 Preparation of Optimized MNP

Preparation of Magnetite (Iron oxide)

The magnetite was prepared using co-precipitation method. The ferrous chloride tetra hydrate (0.5%) solution was maintained between 80 to 90°C and stirred continuously at 1800 rpm by using magnetic stirrer with hot plate. Followed by the ammonia solution was added to the above solution drop wise and the formation of magnetite was indicated by the colour changes from the orange to black. The precipitate was washed with distilled water for 6 times and then filtered and dried overnight [16].

Preparation of quercetin loaded MNP

The MNP was prepared by ionic gelation method. The aqueous solution of sodium tripolyphosphate (1mg/mL) is added drop wise into various concentration of 20 mL of chitosan-acetic acid solution containing 20 mg of magnetite and 10mg of quercetin with constant stirring room temperature for 6 h. Then it was centrifuged at 12000 rpm on 8°C and the supernatant was removed and the precipitate was freeze dried and lyophilized [17].

2.4 Characterization of Optimized MNP

Scanning Electron Microscopy

The surface morphology of the magnetite nanoparticles was studied using a scanning electron microscope (Hitachi, S4800). Prior to SEM observation, the samples were coated with a fine layer of platinum with the help of a JEOL JFC-1100E ion spraying apparatus and secured to the holder using adhesive tape. Using an acceleration voltage of 5 kV and a magnification of between 100 and 150 k, scanning electron pictures were produced [16].

Particle size and Zeta potential

The nanoparticles were dispersed in distilled water and filtered. The resulting filtrate is taken in a quartz cuvette and tested using Anton Paar Litesizer 500. The average hydrodynamic diameter and zeta potential of the MNP was measured.

Drug content

In the above prepared nanoparticles i.e., the total amount of product is about 180mg out of which 40mg is drug. For the evaluation of drug content 1mg of pure drug (Quercetin), and an amount of the prepared formulation equivalent to 1mg of pure drug is taken i.e.,4.5mg. This is dissolved in 100ml of 7.4 phosphate buffer and 1ml was taken from the solution and made the volume was made up to 10ml. The solution was analyzed in UV spectrophotometry (Shimadzu UV-2700i) at a wavelength of 370nm and the drug content is calculated with the help of the calibration curve of quercetin [18].

Drug loading

In the above prepared nanoparticles i.e., the total amount of product is about 180mg out of which 40mg is drug. For the evaluation of drug content 1mg of pure drug (Quercetin), and 1mg of the prepared formulation is taken. This is dissolved in 100ml of 7.4 phosphate buffer and 1ml was taken from the solution and made the volume was made up to 10ml. The solution was analyzed in UV spectrophotometry (Shimadzu UV-2700i) at a wavelength of 370nm and the drug content is calculated with the help of the calibration curve of quercetin [18].

In vitro drug release

To study the drug release profile of quercetin loaded MNPs, drug-loaded nanoparticles dispersed in PBS as described earlier were placed inside dialysis bags. Samples were incubated at room temperature. At designated time intervals, 1 mL of dialysate was removed from each sample and stored at -20° C for later analysis. Dialysate volume was reconstituted by adding 1 mL of fresh PBS to each sample. After the experiment the dialysate samples were analyzed using a UV-Vis spectrometer to determine the amount of quercetin released into the dialysate [19].

Kinetics modelling of in vitro drug release study

To determine the propranolol HCL release kinetics, various drug release kinetic models, such as zero-order kinetics, first-order kinetics with the Higuchi model, and the Korsmeyer-Peppas model, were used [20].

In vitro cytocompatibility study

The in vitro cytocompatibility of the prepared quercetin loaded MNP was analyzed using MTT assay [21]. Briefly MCF-7 cell lines were seeded in 96-well plates aseptically, with the density of cells 2.5x 102cell/well and incubated at 12hr (adhesion periods of the cell). The Samples was concomitantly treated concentration (300 to 0.025Um/MI) incubation at 37°C in 24 hrs, after the cells in each well treated with 10µmol of MTT dye incubation at 37°C for 3hrs in a dark place. Further, the well plate medium was withdrawn and added 150µmol of DMSO (100%) in each well to dissolve the MTT Formosan crystals. Finally, the well plate loaded in a micro plate reader (Multiskan, Thermo scientific) measure the absorbance of each well were documented at a spectral wavelength of 570nm to 590 (n=3).

2.5 Stability study

The quercetin loaded MNP were checked for the stability by incubating at 40°C and 75% RH for 30 days [22]. The stability of the quercetin loaded MNP were determined using the particle size, zeta potential, absorption maxima and drug content before and after 30 days for incubation at 40°C & 75% RH.

3. REPORT AND DISCUSSION

3.1 Design of Experiment

Here, RSM was performed for the MNP to check the effect of three factors such as sodium tripolyphosphate, chitosan, and rotation speed (selected based on the factorial screening) on the responses (particle size and zeta potential). The factors and expected responses range have been represented in table 1&2. Design Expert Software (Version 13.0.1.0) was utilized to evaluate the factors interaction and their effects on the MNP formulation. Totally 17 runs have been performed in accordance to the model design and their results were shown in table 3 and 4.

Facto r	Name	Unit s	Type	Subtype	Minimu m	Maximu m	Coded Low	Coded High	Mean	Std. Dev.
A	Sodium triopoly phospha te	mg	Numer ic	Continuo us	5.00	20.00	-1 ↔ 5.00	+1 ↔ 20.00	12.50	5.30
В	Chitosan	mg	Numer ic	Continuo us	0.5000	5.00	-1 ↔ 0.50	+1 ↔ 5.00	2.75	1.59

Table 1: Levels of independent variables

С	Rotation	rpm	Numer	Continuo	3000.00	5000.00	-1 ↔	+1 ↔	4000.0	707.1
	al speed		ic	us			3000.0	5000.0	0	1
	_						0	0		

Table 2: Levels of dependent variables

Response	Name	Units	Observations	Minimum	Maximum	Mean	Std. Dev.	Ratio
R1	Particle Size	nm	17.00	451.9	503.1	479.54	15.34	1.11
R2	Zeta Potential	mV	17.00	-33	-25	-29.12	2.50	1.32

Table 3: Model design summary

Study type	Response surface methodology
Sub type	Randomized
Design type	Box Behnken
Design model	Quadratic
Runs	17
Blocks	0

Table 4: Experimental runs with responses

		Factor 1	Factor 2	Factor 3	Response 1	Response 2
Std	Run	A: Sodium triopoly phosphate	B: Chitosan	C: Rotational speed	Particle Size	Zeta Potential
		mg	mg	rpm	nm	mV
1	1	5	0.5	4000	466.9	-30
7	2	5	2.75	5000	503.1	-30
14	3	12.5	2.75	4000	458.2	-26
2	4	20	0.5	4000	465.5	-30
4	5	20	5	4000	498.3	-33
17	6	12.5	2.75	4000	464.9	-25
16	7	12.5	2.75	4000	485.8	-27
12	8	12.5	5	5000	477.1	-31
9	9	12.5	0.5	3000	451.9	-25
3	10	5	5	4000	480.3	-28
5	11	5	2.75	3000	492.5	-32

15	12	12.5	2.75	4000	479.1	-30
11	13	12.5	0.5	5000	469.8	-29
6	14	20	2.75	3000	499.2	-27
10	15	12.5	5	3000	496.2	-33
8	16	20	2.75	5000	475.1	-30
13	17	12.5	2.75	4000	488.2	-29

Analysis of Variance (ANOVA) was performed for each response (particle size and zeta potential). The results of ANOVA for particle size and zeta potential were shown in table 5&6 respectively.

Table 5: ANOVA result for particle size of MNP

Source	Sequential p-value	Lack of Fit p-value	Adjusted R ²	Predicted R ²	P-value significance
Linear	0.1509	0.4677	0.1698	-0.2112	
2FI	0.3094	0.4965	0.2341	-0.6248	Not
Quadratic	0.1563	0.7676	0.4574	-0.1459	significant
Cubic	0.7676		0.2652		

Table 6: ANOVA result for zeta potential of MNP

Source	Sequential p-value	Lack of Fit p-value	Adjusted R ²	Predicted R ²	P-value significance
Linear	0.4944	0.3174	-0.0303	-0.4434	
2FI	0.3741	0.3086	0.0054	-0.9098	Not
Quadratic	0.3507	0.2927	0.0847	-2.9180	significant
Cubic	0.2927		0.3104		

Table 5 represents the ANOVA results of response particle size of MNP which indicates the model F-value of 1.16 implies the model is not significant relative to the noise. There is a 43.01% chance that an F-value this large could occur due to noise. P-values less than 0.0500 indicate model terms are significant. In this case there are no significant model terms. Values greater than 0.1000 indicate the model terms are not significant. If there are many insignificant model terms (not counting those required to support hierarchy), model reduction may improve your model. The Lack of Fit F-value of 1.76 implies the Lack of Fit is not significant relative to the pure error. There is a 29.27% chance that a Lack of Fit F-value this large could occur due to noise. Therefore, no significant noise was noticed and the model suits for the experiment in accordance the particle size response.

Table 6 represents the ANOVA results of response zeta potential of MNP which indicates the model F-value of 2.50 implies the model is not significant relative to the noise. There is a 12.03% chance that an F-value this large could occur due to noise. P-values less than 0.0500 indicate model terms are significant. In this case B is a significant model term. Values greater than 0.1000 indicate the model terms are not significant. If there are many insignificant model terms (not counting those required to support hierarchy), model reduction may improve your

model. The Lack of Fit F-value of 0.39 implies the Lack of Fit is not significant relative to the pure error. There is a 76.76% chance that a Lack of Fit F-value this large could occur due to noise. Therefore, no significant noise was noticed and the model suits for the experiment in accordance the zeta potential response.

Perturbation graph were plotted to find those factors that most affects the response. A steep slope or curvature in a factor shows that the response is sensitive to that factor. A relatively flat line shows insensitivity to change in that particular factor. Figure 1 represents the perturbation plot for the particle size of MNP which indicates factor C and A shows a slight slope implying that it has a significant effect on the response, factors B has a significance influence on particle size. Figure 2 represents the perturbation plot for the zeta potential of MNP which indicates factor A, B and C shows a steep slope implying that it has a significant effect on the response.

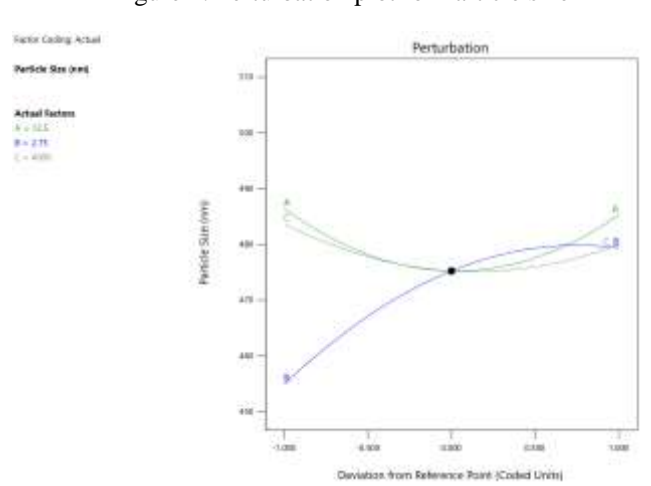
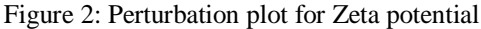
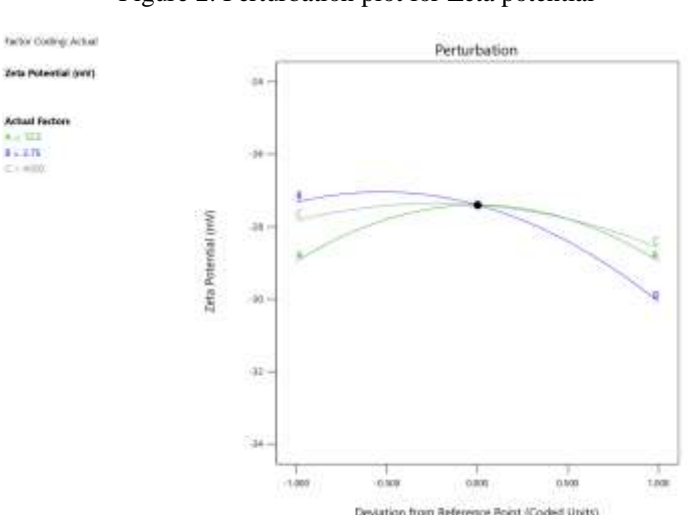


Figure 1: Perturbation plot for Particle size





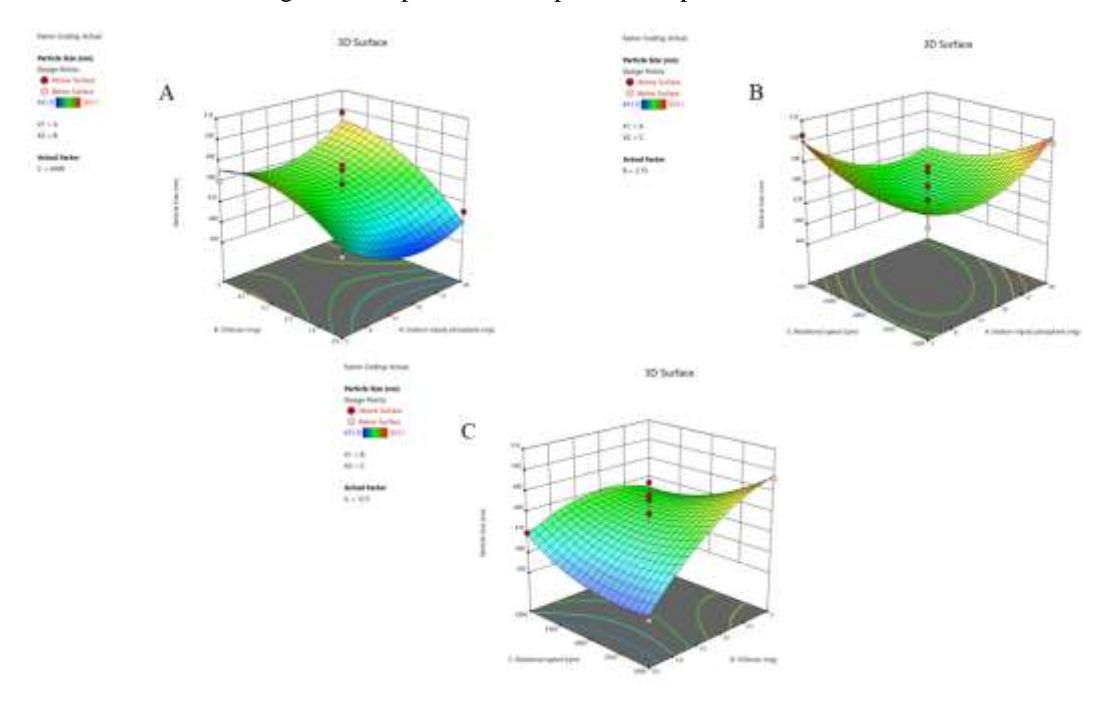


Figure 3: Response surface profiles for particle size of MNP

Figure 3 represents the response surface profiles for the particle size of MNP in respect to the effects of factors as an individual and combined. Figure 3A indicates the increase in the concentration of chitosan and sodium tri polyphosphate causes decrease in particle size. Figure 3B indicates the increase in sodium tripolyphosphate and decrease in the rotational speed causes increase in the particle size. Figure 3C represent the increase in the rotational speed and concentration of chitosan leads to the decrease in particle size.

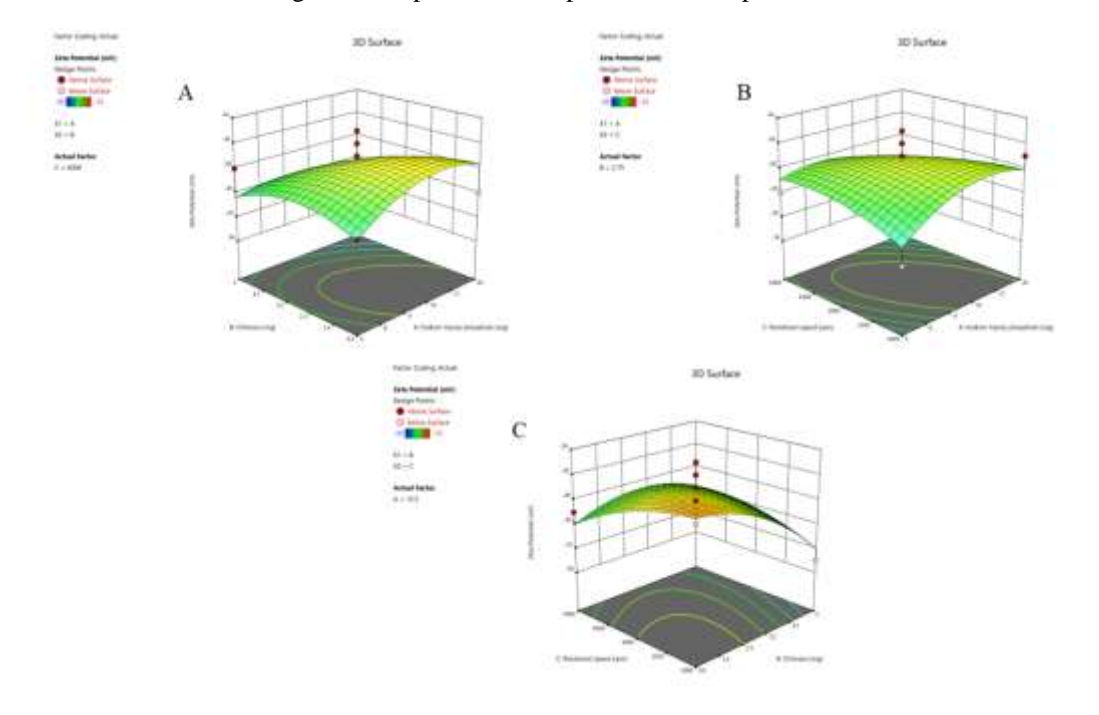


Figure 4: Response surface profiles for zeta potential of MNP

Figure 4 represents the response surface profiles for the zeta potential of MNP in respect to the effects produced by the factors as an individual and combined. Figure 4A indicates the increase in the concentration of chitosan and sodium tri polyphosphate leads to the reduction in zeta potential of MNP. Figure 4B indicates the increase in sodium tripolyphosphate and increase in the rotational speed leads to increase in the zeta potential. Figure 4C

indicates the decrease in the rotational speed and concentration of chitosan causes the reduction in the zeta potential of MNP.

A Solar transportant regular r

Figure 5: Graph for desirability prediction (Contour Plot)

Here, we used desirability tabulation used to optimize the formulation factors (Figure 5). From the above plot, we can conclude that the zeta potential of ideal concentration of sodium tripolyphosphate lies between 8mg to 15mg and in the case of chitosan it lies between 2 to 4 mg. The optimized formula for the formulation was shown in table 7.

Sodium SD for **Predicted Predicted** SD for zeta Rotation Chitosan particle tripoly zeta particle size potential speed phosphate size potential 4500rpm 484.3 ± 21.2 -26.8 ±5.1 15mg 2mg

Table 7: Optimized formula for MNP

3.2 Preparation of magnetite

The magnetite was prepared using co-precipitation method as per the procedure mentioned above. The magnetite precipitate was filtered and dried overnight. A magnetic bead was used for the confirmation of magnetite and it was confirmed that the prepared substance was magnetite (Figure 6).



Figure 6: Magnetite confirmation

3.3 Preparation of Optimized MNP

MNP was prepared with the optimized formula predicted by the DOE. The MNP was prepared by ionic gelation method. 15ml of aqueous solution of sodium tripolyphosphate (1mg/mL) is added drop wise into various concentration of 20 mL of chitosan-acetic acid (2mg/ml) solution containing 20 mg of magnetite and 10mg of quercetin with constant stirring at 4500 rpm in room temperature for 6 h. Then it was centrifuged at 12000 rpm

on 8°C and the supernatant was removed and the precipitate was freeze dried and lyophilized. The drug powder of quercetin was prepared and stored for further studies.

3.4 Characterization of Optimized MNP

Scanning Electron Microscopy

The information on the microscopic features of the surface topography, size, and shape of the particles, as well as properties of the MNP, is revealed by the SEM studies [23]. The SEM of quercetin loaded MNP (figure 7) was crystalline shape.

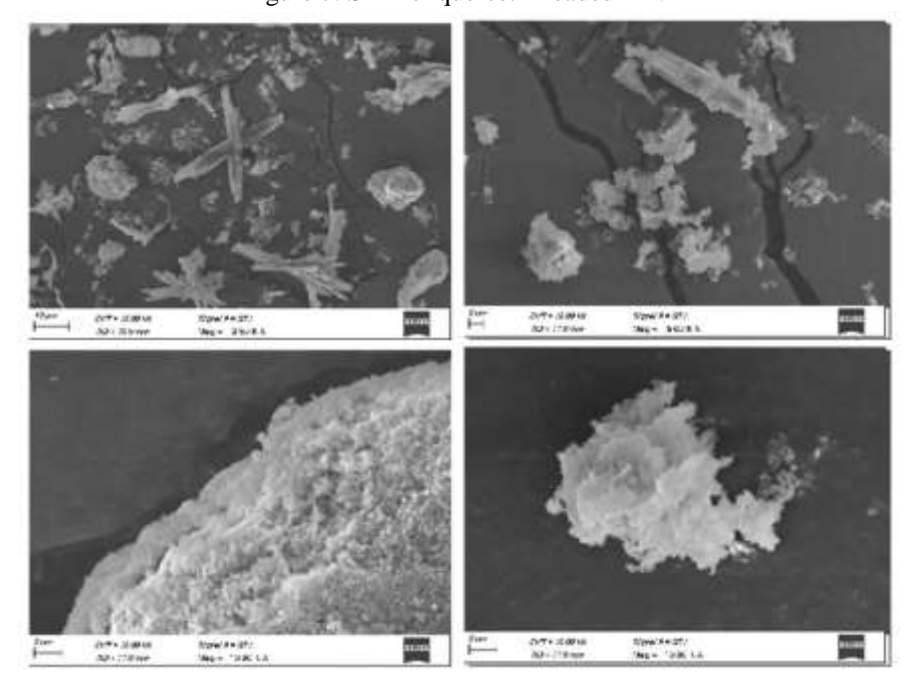


Figure 7: SEM of quercetin loaded MNP

Particle size and Zeta potential

The particle size and zeta potential of the quercetin loaded optimized MNP were determined using Anton Paar Litesizer 500. The optimized quercetin loaded MNP shows the particle size of 489.5±12.7nm (Figure 8) and zeta potential of -25.3±1.5mV (Figure 9). The observed particle size and zeta potential were under the range of responses predicted by DOE.

Figure 8: Particle size of optimized quercetin loaded MNP

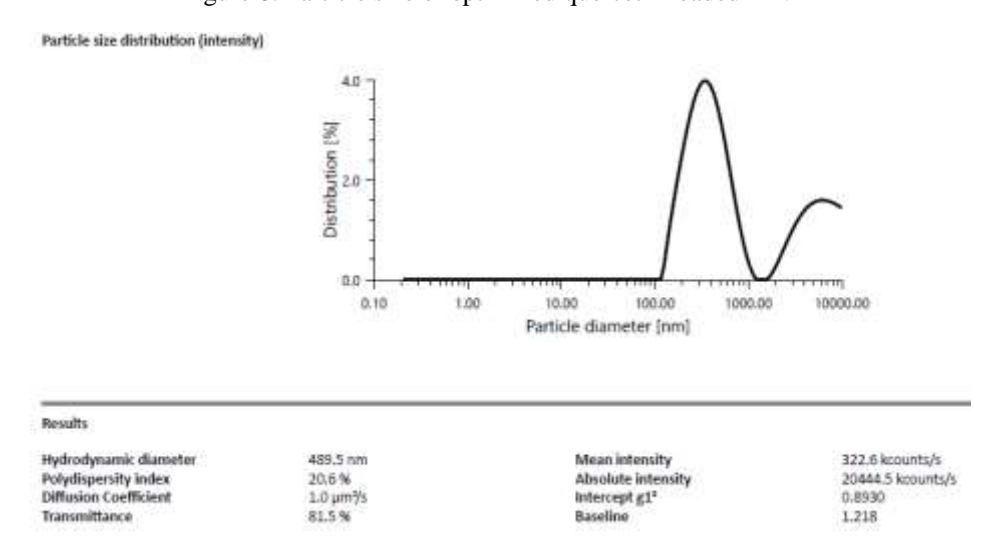
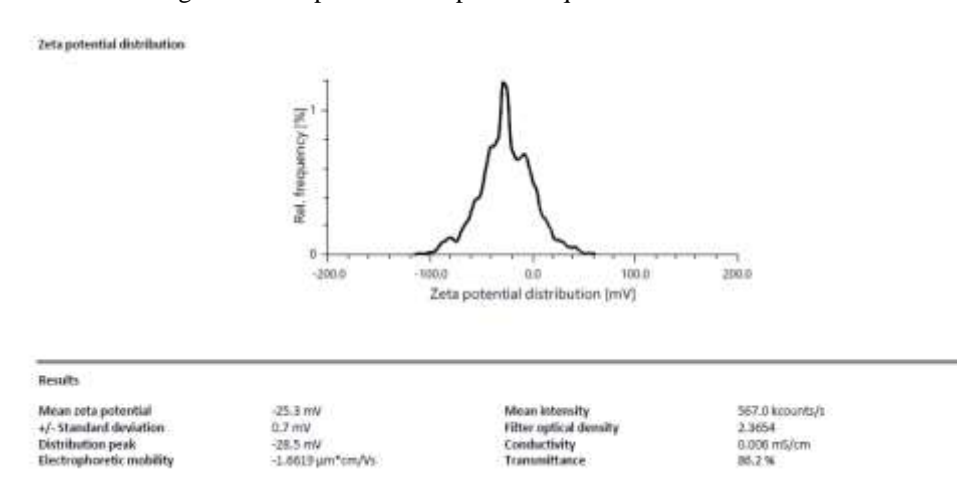


Figure 9: Zeta potential of optimized quercetin loaded MNP



Drug content

4.5mg of quercetin loaded MNP was taken and dissolved in 100ml of 7.4 phosphate buffer and 1ml was taken from the solution and made the volume was made up to 10ml. The solution was analysed in UV spectrophotometry at a wavelength of 370nm and the drug content was found to be 94%.

Drug loading

1mg of prepared quercetin loaded MNP was taken and dissolved in 100ml of 7.4 phosphate buffer and 1ml was taken from the solution and made the volume was made up to 10ml. The solution was analysed in UV spectrophotometry at a wavelength of 370nm and the drug loading was found to be 21.77% of quercetin in mg of MNP.

In vitro drug release

The in vitro drug release of the quercetin from the MNP was performed using dialysis method. The in vitro release profile of prepared formulation was represented in figure 10. Initially, there was burst release and followed by sustained release of quercetin from the MNP. At 80th minute, the drug release was 48.55% and 99.35% drug release by 5180th minute.

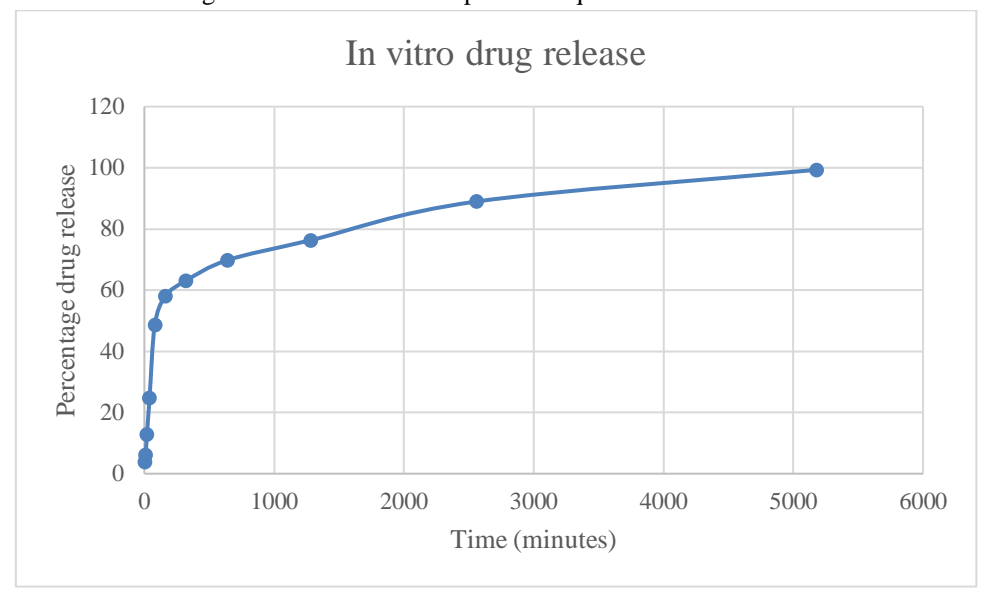


Figure 10: In vitro release profile of quercetin loaded MNP

Kinetics modelling of in vitro drug release study

The different kinetics such as zero order (Fig.11A), Higuchi model (Fig.11B), Korsmeyer peppas model (Fig.11C), first order (Fig.11D) and Hixson Crowell model (Fig.11E) for in vitro drug release were shown in figure 11 and was interpreted in table 8. The study found that drug release follows first order release kinetics with a R2 value of 0.9564, which indicates that the in vitro release of MNP follows first order release. It was best fitted with the Korsmeyer-Peppas model (R2 value 0.9497) with a n value of 0.734, indicating a non-fickian super case II type of release mechanism [24].

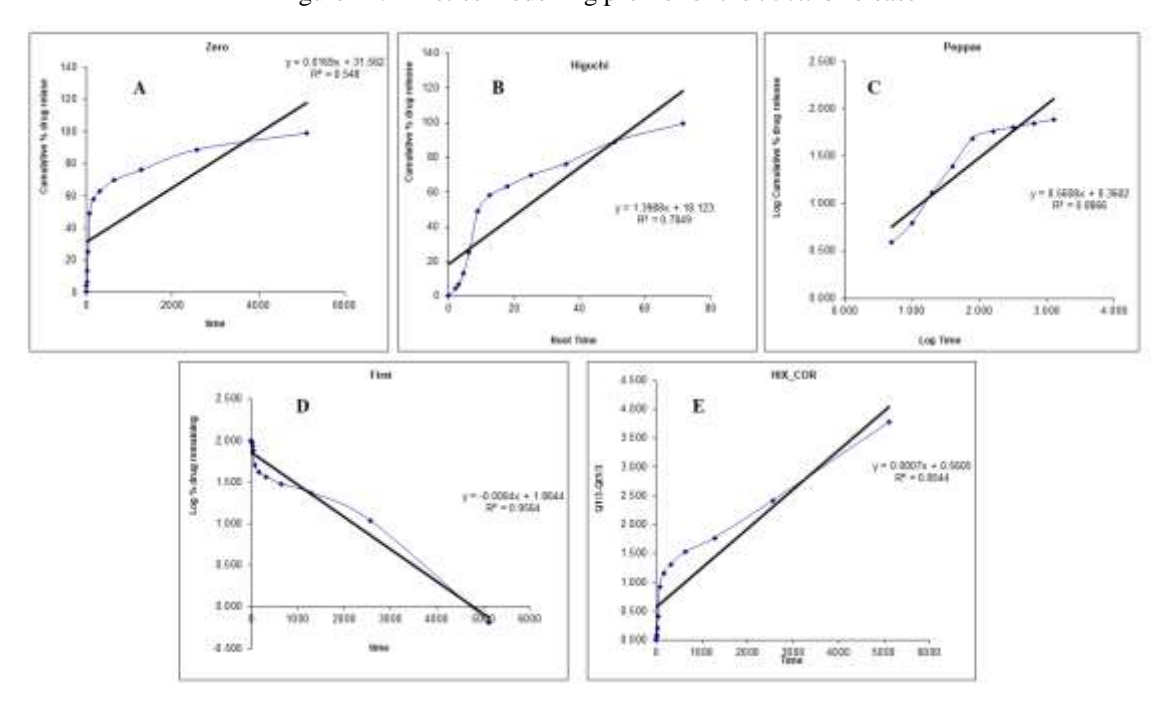


Figure 11: Kinetics modelling profile for the *in vitro* release

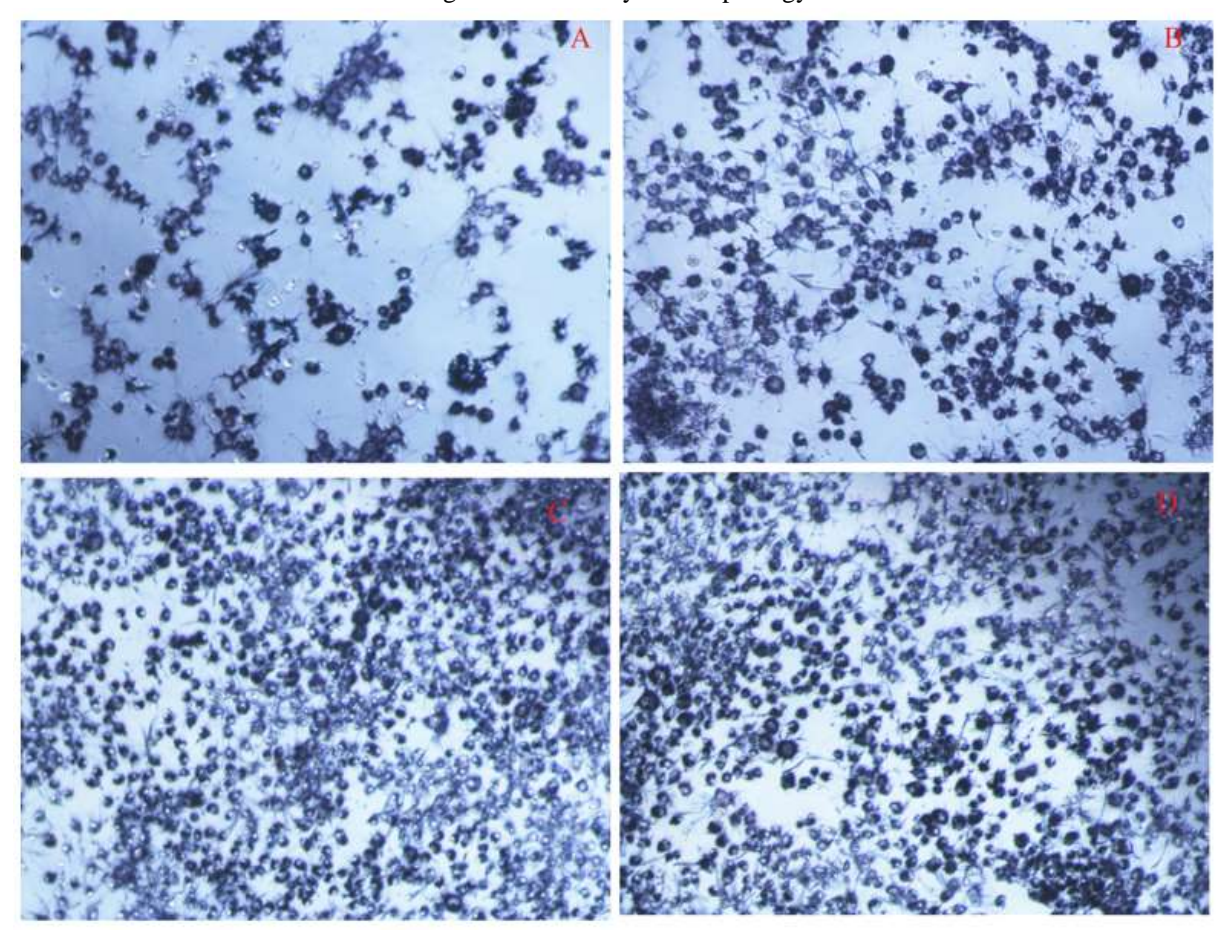
Table 8: Kinetics model interpretations

S. No	Zero	Higuchi	Peppas		First	Hix-cro
2.2.0		8	\mathbb{R}^2	n		
1.	0.5480	0.7849	0.9497	0.734	0.9564	0.844

Cell culture

The in vitro cytocompatibility was performed on MCF-7 cell lines with three samples (blank formulation, control quercetin and quercetin loaded MNP). The samples were concomitantly treated concentration (300 to 0.025 Um/Ml) incubation at 37°C in 24 hrs, after the cells in each well treated with $10\mu\text{mol}$ of MTT dye incubation at 37°C for 3hrs in a dark place. The MTT Formosan crystals (figure 12) was dissolved using DMSO and absorbance were noted for the spectral range of 570-590nm. The figure 13 shows live and dead MCF-7 cells with samples. The IC 50 study was performed with the samples in that blank MNP has IC 50 value was $20\mu\text{g/ml}$ whereas the control quercetin and quercetin loaded MNP were $33\mu\text{g/ml}$ & $32\mu\text{g/ml}$ respectively. The IC 50 values portraits that the quercetin loaded MNP shows significant compatibility with MCF-7 cells as like control quercetin in comparison to the blank MNP.

Figure 12: MTT crystal morphology



Tigure 13. Elve de dedu cens

Figure 13: Live & dead cells

3.5 Stability study

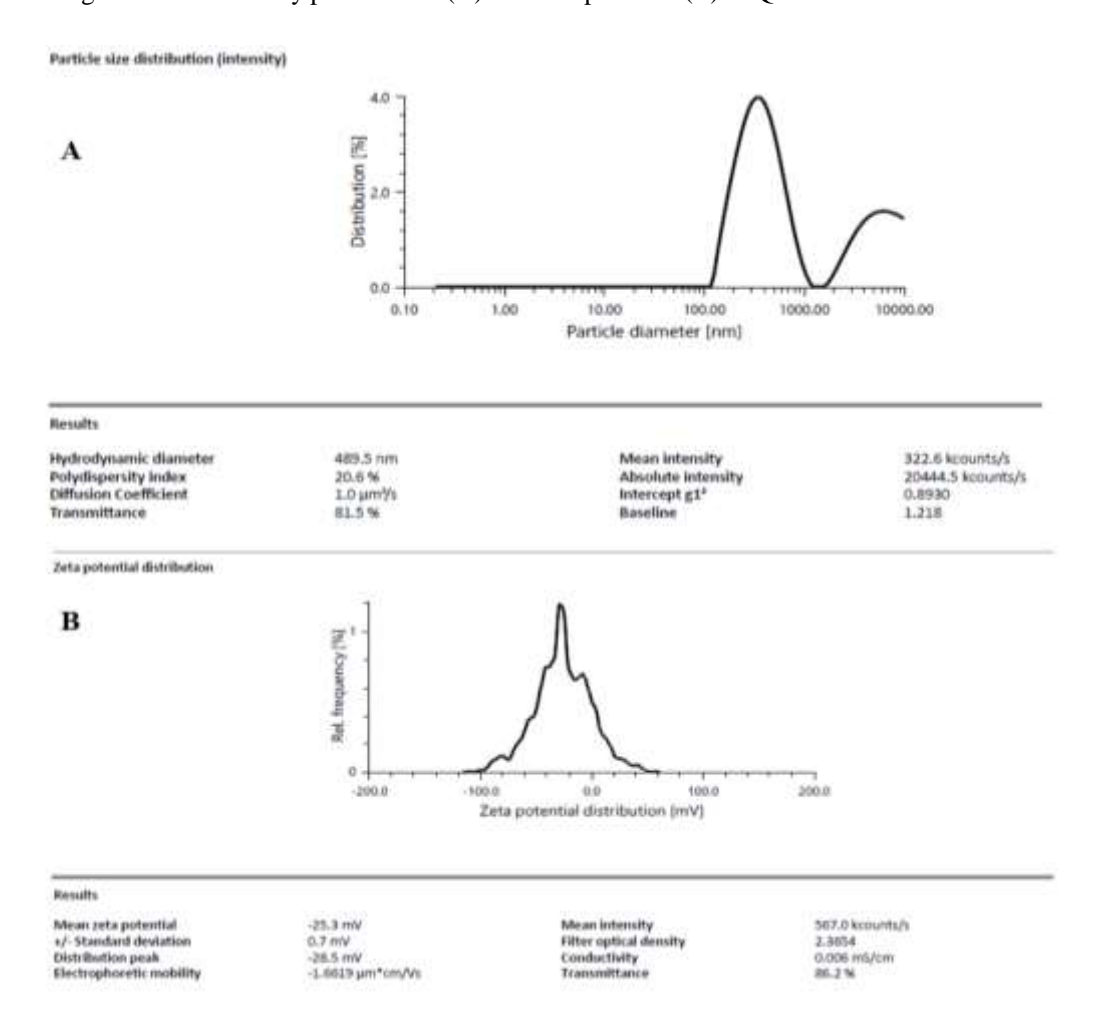
Pre stability studies

The absorption maxima, drug content, particle size (figure 14 A) and zeta potential (figure 14 B) of the quercetin loaded MNP were analysed before performing the stability testing. The observation of the tests was shown in the table 9.

Table 9: Pre stability results

Tests	Observation
Лmax	365.3nm
Drug content	94%
Particle size	489.5nm
Zeta potential	-25.3mV

Figure 14: Pre stability particle size (A) and zeta potential (B) of Quercetin loaded MNP



Post stability studies

The absorption maxima, drug content, particle size (figure 15 A) and zeta potential (figure 15 B) of the quercetin loaded MNP were analysed after performing the stability testing. The observation of the tests was shown in the table 10.

Table 10: Post stability results

Tests	Observation
́лмах	379.8nm
Drug content	92%
Particle size	499.5nm
Zeta potential	-27.9mV

Particle size distribution (intensity) 4.0 A Æ Distribution (0.10 Particle diameter (nm) 499.5 nm 322.6 kcounts/s 20.6 % 1.0 µm²/s 81.5 % Polydispersity index Diffusion Coefficient Absolute inte 20444.5 konunts/s Intercept g1³ Baseline 1.218 Zeta potential distribution B Zeta potential distribution [mV] Mean zeta potential 27.9 mV 567,0 kcounts/s +/- Standard deviation Distribution peak 0.8 mV -21.2 mV Filter optical de Conductivity 2.6336 0.005 m3/cm -1.7655 µm*cm/Vs Electrophoretic mobility Trommittance 87.0 %

Figure 15: Pre stability particle size (A) and zeta potential (B) of Quercetin loaded MNP

4. CONCLUSION

This study demonstrated the use of quercetin-loaded MNP for the treatment of MBC by delivering the medicine to the barriers. In this study, we used the ionic gelation method to manufacture and analyse quercetin-loaded MNP. By applying DOE to connect the independent variables with the results of 17 trials, the formulation was optimised. The DOE's optimal formulation was modified for convenience, and quercetin-loaded MNP were created. According to the DOE prediction profile, the improved MNP was able to produce the repeatable predetermined responses (particle size, zeta potential, and PDI). The developed MNP formulation's physiochemical characterisation was found to be sufficient. The *in vitro* drug release study showed an initial release followed by a sustained drug release and the kinetics of the *in vitro* release was calculated. The *in vitro* compatibility with MCF-7 cells showed that the quercetin loaded MNP was compatible and IC50 value was similar to the control quercetin whereas the blank MNP was less compared to the quercetin loaded MNP. The prepared quercetin loaded MNP was stable for 30 days in accelerated condition.

ACKNOWLEDGEMENT

We would like to express our sincere gratitude to Amity Institute of Pharmacy, Amity University, for all the guidance and support.

Conflicts of interest: The authors have no conflicts of interest.

Authors funding: Not applicable.

REFERENCE

- 1. Tosello G, Torloni MR, Mota BS, Neeman T, Riera R. Breast surgery for metastatic breast cancer. Cochrane Database of Systematic Reviews. 2018(3).
- 2. Peart O. Metastatic breast cancer. Radiologic technology. 2017 May 1;88(5):519M-39M.
- 3. Chen MT, Sun HF, Zhao Y, Fu WY, Yang LP, Gao SP, Li LD, Jiang HL, Jin W. Comparison of patterns and prognosis among distant metastatic breast cancer patients by age groups: a SEER population-based analysis. Scientific reports. 2017 Aug 23;7(1):1-8.
- 4. Spazzapan S, Crivellari D, Bedard P, Lombardi D, Miolo G, Scalone S, Veronesi A. Therapeutic management of breast cancer in the elderly. Expert Opinion on Pharmacotherapy. 2011 Apr 1;12(6):945-60.
- 5. Wen L, Zhao Y, Jiang Y, Yu L, Zeng X, Yang J, Tian M, Liu H, Yang B. Identification of a flavonoid C-glycoside as potent antioxidant. Free Radical Biology and Medicine. 2017 Sep 1;110:92-101.
- 6. Ezzati M, Yousefi B, Velaei K, Safa A. A review on anti-cancer properties of Quercetin in breast cancer. Life Sciences. 2020 May 1;248:117463.
- 7. Fang X, Cao J, Shen A. Advances in anti-breast cancer drugs and the application of nano-drug delivery systems in breast cancer therapy. Journal of Drug Delivery Science and Technology. 2020 Jun 1;57:101662.
- 8. Kumar SR, Priyatharshni S, Babu VN, Mangalaraj D, Viswanathan C, Kannan S, Ponpandian N. Quercetin conjugated superparamagnetic magnetite nanoparticles for in-vitro analysis of breast cancer cell lines for chemotherapy applications. Journal of colloid and interface science. 2014 Dec 15;436:234-42.
- 9. Majewski P, Thierry B. Functionalized magnetite nanoparticles—synthesis, properties, and bioapplications. CRC Press; 2008 Dec 22.
- 10. Calero M, Chiappi M, Lazaro-Carrillo A, Rodríguez MJ, Chichón FJ, Crosbie-Staunton K, Prina-Mello A, Volkov Y, Villanueva A, Carrascosa JL. Characterization of interaction of magnetic nanoparticles with breast cancer cells. Journal of nanobiotechnology. 2015 Dec;13(1):1-5.
- 11. B. Singh, S.K. Chakkal, N. Ahuja. Formulation and optimization of controlled release mucoadhesive tablets of atenolol using response surface methodology. AAPS PharmSciTech. 2006;7:1–10.
- 12. Mujtaba, M. Ali, K. Kohli. Formulation of extended release cefpodoxime proxetil chitosan-alginate beads using quality by design approach. Int. J. Biol. Macromol. 2014;69:420–429.
- 13. D. Soans, R. Chandramouli, A.N. Kavitha, S.K. Roopesh, S. Shrestha. Application of design of experiments for optimizing critical quality attributes (CQA) in routine pharmaceutical product development. J. Pharm. Res. 2016;15:96.
- 14. Ferreira SC, Bruns RE, Ferreira HS, Matos GD, David JM, Brandão GC, da Silva EP, Portugal LA, Dos Reis PS, Souza AS, Dos Santos WN. Box-Behnken design: an alternative for the optimization of analytical methods. Analytica chimica acta. 2007 Aug 10;597(2):179-86.
- 15. R. Calfee, D. Piontkowski. Design and analysis of experiments, Handb. Read. Res. 2016; 63-90.
- 16. Petcharoen K, Sirivat AJ. Synthesis and characterization of magnetite nanoparticles via the chemical co-precipitation method. Materials Science and Engineering: B. 2012 Mar 25;177(5):421-7.
- 17. Furtado GT, Fideles TB, Cruz RD, Souza JW, Rodriguez Barbero MA, Fook MV. Chitosan/NaF particles prepared via ionotropic gelation: evaluation of particles size and morphology. Materials Research. 2018 Jun 25;21.
- 18. Numata Y, Tanaka H. Quantitative analysis of quercetin using Raman spectroscopy. Food Chemistry. 2011 May 15;126(2):751-5.
- 19. Rahimi M, Wadajkar A, Subramanian K, Yousef M, Cui W, Hsieh JT, Nguyen KT. In vitro evaluation of novel polymer-coated magnetic nanoparticles for controlled drug delivery. Nanomedicine: Nanotechnology, Biology and Medicine. 2010 Oct 1;6(5):672-80.
- 20. Ghosh S, Kokot-Blamey J, Boot-Handford ME, Fennell PS. Kinetics modeling, development, and comparison for the reaction of calcium oxide with steam. Energy & Fuels. 2019;33:5505-17.
- 21. Askari A, Tajvar S, Nikkhah M, Mohammadi S, Hosseinkhani S. Synthesis, characterization and in vitro toxicity evaluation of doxorubicin-loaded magnetoliposomes on MCF-7 breast cancer cell line. Journal of Drug Delivery Science and Technology. 2020 Feb 1:55:101447.
- 22. Fitzpatrick S, McCabe JF, Petts CR, Booth SW. Effect of moisture on polyvinylpyrrolidone in accelerated stability testing. International Journal of Pharmaceutics. 2002 Oct 10;246(1-2):143-51.
- 23. Sundrarajan M, Ramalakshmi M. Novel cubic magnetite nanoparticle synthesis using room temperature ionic liquid. E-Journal of Chemistry. 2012 Jan 1;9(3):1070-6.
- 24. Trongchuen K, Ounkaew A, Kasemsiri P, Hiziroglu S, Mongkolthanaruk W, Wannasutta R, Pongsa U, Chindaprasirt P. Bioactive starch foam composite enriched with natural antioxidants from spent coffee ground and essential oil. Starch-Stärke. 2018 Jul;70(7-8):1700238.